Supplementary Information

Multi-enzyme cascade reactions using protein-polymer surfactant self-standing films

Thomas Farrugia[†], Adam W. Perriman[#], Kamendra P. Sharma[†¶], and Stephen Mann[†*]*

[†]Centre for Organized Matter Chemistry and Centre for Protolife Research, School of Chemistry, University of Bristol, BS8 1TS, United Kingdom.

[#]School of Cellular and Molecular Medicine, University of Bristol, BS8 1TD, United Kingdom.

[¶] Department of Chemistry, Indian Institute of Technology Bombay, Powai, Mumbai -400076, India.

Table of Contents:

1. Experimental:

i. Materials:

3-(Dimethylamino)-1-propylamine (DMAPA; D145009), 50 wt% in H_2O glutaraldehyde, (340855), Poly(ethylene glycol) 4-nonylphenyl 3-sulfopropyl ether (**S_1**; 473197, 2,2′-Azino-bis(3-ethylbenzothiazoline-6-sulfonic acid) diammonium salt (ABTS; A1888, D-Glucose (G5767), 30 wt% Hydrogen Peroxide (216763), Glucose Oxidase (100-250 Kilounits/g) (GOx, G7141), ß-Glucosidase (>6Units/mg) (BGL, 49290) and horseradish peroxidase (150 Units/mg) (HRP, Prod. No: 77332) were purchased from Sigma Aldrich. p-Nitrophenyl-β-D-glucopyranoside (PNPG, Prod.No: 303110010) was purchased from Acros Organics. N-(3-Dimethylaminopropyl)-N'-ethylcarbodiimide hydrochloride (EDC.HCl, FD05800) was purchased from Carbosynth Ltd. All chemicals were used as supplied.

ii. Preparation of protein-polymer surfactant nanoconjugates and hybrid films:

(a) Protein cationization: Aspartic and glutamic acid residues on proteins were cationized using an EDC zero-length crosslinker and either DMAPA or HMDA as the cationizing amine. Generally the amine was diluted to a concentration of 200 mg ml^{-1} and then brought to pH 6 using HCl (6M), after which it was added to a solution of native protein dissolved in MilliQ grade (18.2 $M\Omega^{-1}cm^{-1}$) water, bringing the final protein concentration to 5 $mgml^{-1}$. A 50-fold excess of EDC.HCl was then added to the solution, and added twice more at hourly intervals to maintain the reaction. The reaction pH was maintained at pH 6 at hourly intervals for the first 3 hours, after which the reaction proceeded overnight. The protein was subsequently dialyzed against MilliQ grade water with frequent water changes over a 48 hour period. Aggregates were removed using a 0.22 µm syringe filter, and the resulting solutions lyophilized. The degree of cationization was determined using MALDI Time of Flight (ToF) mass spectrometry.

*(b) Bioconjugation using **S_1** and formation of nanoclusters*: Formation of **S_1**-c-protein conjugates was achieved by slow addition of a solution of **S_1** ($50mgml^{-1}$) to a stirred solution of aqueous cationized protein (8-10 $mgml^{-1}$). A constant rate of **S_1** addition was ensured using a syringe pump set to 200 $\mu Lmin^{-1}$. Bioconjugate cluster formation was indicated by increasing solution turbidity, and confirmed using dynamic light scattering.

(c) Films Production: Films of bioconjugated proteins were produced by drying the respective solutions in Petri Dishes or optical glass grade cuvettes (Hellma 3.5ml OG 6030). Drying was performed using a silica bead vacuum desiccator that contained 50 wt%

glutaraldehyde, the vapour of which served as a crosslinking agent. A vacuum of -25 mm Hg was applied to the desiccator to facilitate drying, after which it was sealed for 48 to 72 hours. Films produced in Petri Dishes were detached by addition of MilliQ Grade water, whereas films cast into cuvettes were used directly for assays. Production of two and three enzyme films was achieved by mixing solutions of the respective bioconjugate proteins under stirring conditions, and then dispensing the required volume of mixture into cuvettes or petri dishes.

iii. *Enzyme assays:*

Michaelis-Menten assays of native, cationized or bio-conjugated proteins, and hybrid protein-polymer surfactant film were performed on a Lambda 25 UV-Vis spectrophotometer equipped with a Peltier temperature controller and a magnetic stirring device. Rates of reaction were monitored using chromogenic substrates (ABTS; 414, 730 nm) and PNPG (400 nm). In all cases, assays were carried out at pH 6 in 250 mM phosphate buffer at 25°C. HRP assays were carried out in the presence of 3 mM ABTS with a variable H_2O_2 concentration ranging from 25 to 250 uM. GOx was assayed in the presence of 2.5 mM ABTS and 0.016 mg mL^{-1} HRP solution (150 units/mg) with a variable glucose concentration ranging from 0 to 75 mM and 0 to 150 mM for the **S_1**-cGOx and **S_1**-cGOx/**S_1**-cHRP films, respectively. Stirrer bars were used when studying the film reaction kinetics so as to minimize diffusion limitations. Concentrations of the native and cationized proteins were determined using UV-visible spectroscopy, and those of the bioconjugates were determined by accounting for the volume of **S_1** added to the cationized protein of known concentration. The enzyme concentration in the films was determined by dividing the mass of protein present in the cuvette by the volume of the reaction solution. Initial rates were taken by fitting the curve obtained from 0-10 seconds to the Michaelis Menten function provided in Origin 2015. Fits for the film were only considered if the R^2 value exceed 0.95, so as to account for minor variations in reaction conditions and the film.

Temperature-dependent studies of the 3-enzyme films were performed at 25 and 37 °C using a solution comprised of 250 mM pH 6 phosphate buffer, 2 mM ABTS and 5 mM PNPG. The solution was scanned from 390 to 800 nm at 10 minute intervals over a period of 14 hours, so as to assess the rate of reaction.

*iv. ON-OFF switching of the **S**$_1$-cGOx/**S**$_1$-cHRP films*

ON-OFF switching of the **S**$_1$-cGOx/**S**$_1$-cHRP film was performed in a cuvette at pH 6 and 37 °C. The reaction solution comprised 250 mM glucose, 5 mM ABTS and 33 mM phosphate buffer in a total volume of 3 mL. The film was first soaked thoroughly in phosphate buffer, after which it was handled using reverse tweezers. Initially the film was immersed for 10 minutes, after which it was removed for 10 minutes (during which it was washed multiple times with water and left to partially dry), this being repeated 6 times. UV-Vis absorption readings were taken every 2.5 minutes.

v. Characterization:

(a) Fourier transform infrared spectroscopy (FTIR): Produced films were scanned on an attenuated total resistance FTIR (Perkinelmer 100 with a universal ATR accessory). ATR-FTIR Samples were prepared by removing a piece of film and leaving it to dry on top of the ATR lens.

(b) Scanning Electron Microscopy (SEM)); Field emission SEM (FE-SEM) was performed using a JEOL Field Emission Gun SEM 6330. SEM samples were prepared overnight and left to dry on an aluminium SEM stub in a dessicator.

(c) Dynamic Light Scattering (DLS): DLS experiments of the aqueous native, cationized and bioconjugate solutions were performed on a Malvern Zetaseizer Nano-ZS. The solutions were transferred to empty cuvettes containing water and their volume intensity % collected.

(d) Diffuse reflectance UV-Vis spectroscopy: Diffuse UV-Vis spectra of the films (Fig. S7) were achieved by scanning films that were sandwiched between square quartz plates. All of **S**$_1$-cGOx/**S**$_1$-cHRP, **S**$_1$-cGOx and **S**$_1$-cHRP films were scanned using a peltier equipped Lambda 35 UV-Vis spectrophotometer.

(e) Circular Dichroism: Temperature dependent synchrotron radiation circular dichroism (SRCD) data was collected at beamline B23 at DIAMOND light source, with a wavelength range of 180-260 nm, integration time of 2 seconds and data interval of 1 nm. A vertical geometry setup that included a modified Linkam thermal stage for temperature regulation was used to study the films, which were cast directly onto synthetic quartz plates and dried and crosslinked using a vacuum desiccator. The sample path length was calculated by assuming that films had a uniform thickness equivalent to a monolayer of protein bioconjugate clusters (0.15 μm). Protein concentration was calculated by considering the mass of protein present in the initial droplet, which was then dried to form the film of a given volume. An initial protein-bioconjugate concentration of 0.5 $mgml^{-1}$ yielded a film concentration of 531 $mgcm^{-3}$. SRCD spectra of native and cationized proteins were also recorded using the same parameters, albeit

in liquid cell cuvettes with pathlength 0.02 cm with a horizontal stage geometry and different peltier.

SRCD spectra were background corrected and normalized prior to being deconvoluted using the DICHROWEB[1] service with the CDSSTR algorithm and associated data set, so as to obtain the relative percentages of secondary structure. Spectra were fitted between 190 and 240 nm, and resultant fits were only considered if the normalized root mean square deviation did not exceed 0.06.

(f) MALDI Time of Flight (ToF) Mass Spectrometry: MALDI ToF mass spectra were collected using an UltrafleXtreme ToF mass spectrometer. Samples of native and cationized proteins were run in a dihydroxyacetophenone (DHAP) and diammonium hydrogen citrate (DAHC) matrix which also incorporated 1% triflouroacetic (TFA) acid. In all cases the ratio between protein, TFA and DHAP/DHAC mix was kept at 1:1:1.

2. Figures:

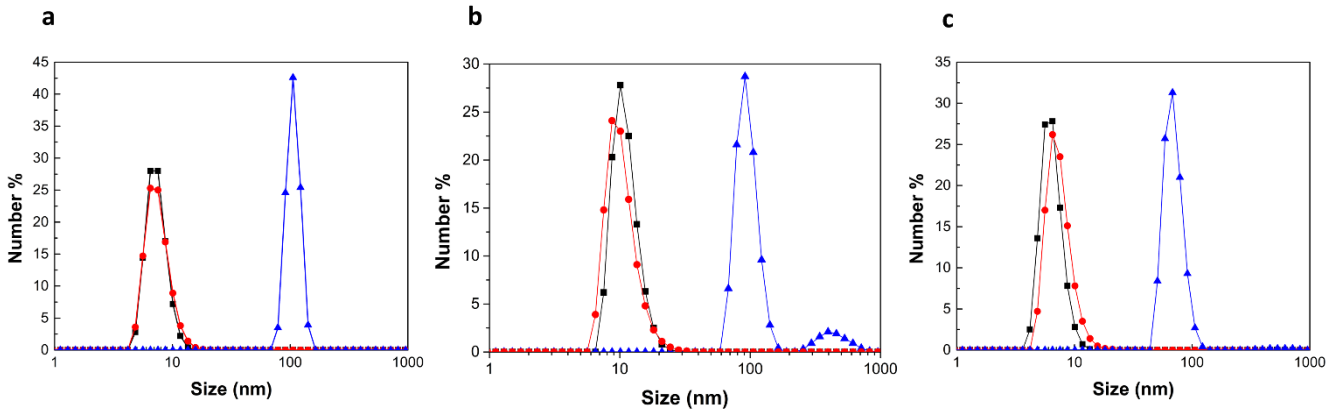

Figure S1: Dynamic Light Scattering (DLS) of solutions of native (black squares), cationized (red squares) and bioconjugated (blue triangles) (a) BGL, (b) GOx, and HRP, respectively showing a large population of ~ 100 nm clusters after electrostatic neutralization with polymer surfactant, $\mathbf{S_1}$.

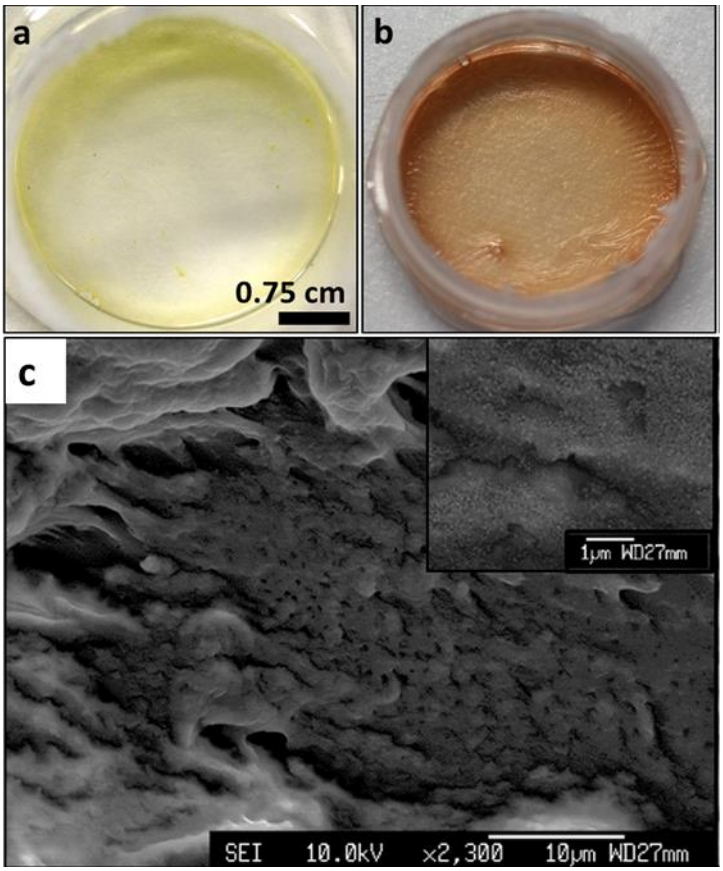

Figure S2: Digital photographs of single enzyme (a) $\mathbf{S_1}$-cGOx, and (b) $\mathbf{S_1}$-cHRP films. (c) SEM Image of $\mathbf{S_1}$-cHRP film, showing cross-linked micron-sized particles assembled from the sub-micron sized (~ 100 nm as obtained from DLS data in **Figure S1**) protein-surfactant polymer clusters (inset).

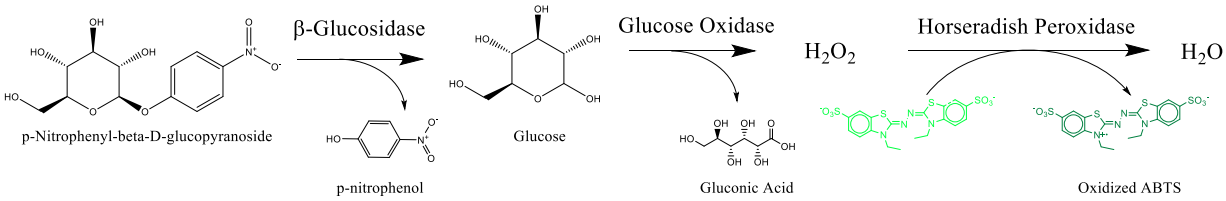

Figure S3: Three enzyme cascade comprising β-glucosidase (BGL), glucose oxidase (GOx), and horseradish peroxidase (HRP) as shown in **Figure 1a** (Schematic) in the main manuscript.

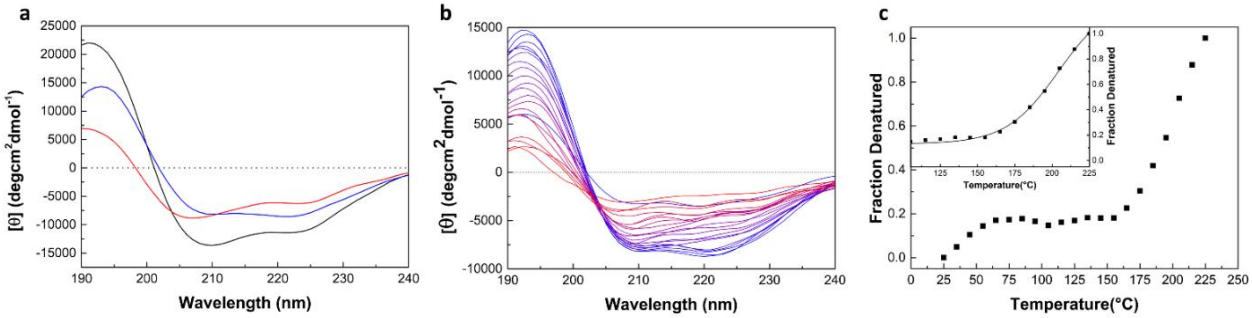

Figure S4: (a) SRCD spectra of GOx and HRP dual mixture in their native (black), cationized (red) and bio-conjugates film (blue) form, recorded at 35°C. (b) Thermal denaturation SRCD spectra of the dual **S_1**-cGOx/**S_1**-cHRP dry film acquired over a temperature range of 25 (blue) to 215°C (red) indicated a progressive decrease in the peak minima and maxima at 208/222 and 195 nm, respectively. Deconvolution of the spectra showed a sharp decrease in the α-helical content from 29% at 25°C to 6% at 215°C, along with a corresponding increase in ß-sheet and unordered domains, which increased from 26% and 32% at 25°C to 28% and 52% at 215°C, respectively. This could be due to gradual loss of secondary structure in both HRP and GOx proteins which is in accord with the temperature denaturation of individual enzymes (**Figure S7c, and Table S3**). (c) Plot of equilibrium fraction of denatured bio-conjugate film as a function of temperature. Use of the peak at 222 nm as an order parameter enabled definition of the fraction of denatured bio-conjugated protein within the film as a function of temperature. The obtained curve (**inset**) shows a plateau from 75 to 150 °C, after which the denaturation occurs in a linear fashion, indicating progressive loss of protein structure. These observations were similar to the T_m observed for single enzyme HRP film (**Figure S8c)** and solvent-free melts produced using similar technique.[2]

Protein	Protein form	α-Helicity	β-sheet	Turns	Unordered
S₁-cGOx/ **S₁**-cHRP (35°C)	Native	41%	16%	16%	28%
	Cationized	19%	22%	17%	41%
	Film	28%	22%	18%	33%

Table S1: Domain content obtained by deconvolution of the spectra in **Figure S4**, corresponding to the aqueous precursors and **S₁**-cGOx/**S₁**-cHRP film. There is a gradual decrease in α-helical content on protein cationization and bioconjugation, with a corresponding increase in all other domains, indicating some structural alteration.

Sample	T_m/°C	Δ*H* (170°C)/ kJ mol^{-1}	Δ*S* (170°C)/ JK^{-1} mol^{-1}	Δ*S* (73°C)/ JK^{-1} mol^{-1}	*T*Δ*S* (73°C)/ kJ mol^{-1}	Δ*G* (73°C)/ kJ mol^{-1}	Δ*H* (73°C)/ kJ mol^{-1}
S₁-cGOx/**S₁**-cHRP film	170	90	203	116	40.3	4.7	45.0
nGOx-nHRP aq. mixture	73	--	--	890	308	0	308

Table S2: Thermodynamic parameters Δ*G*, Δ*H*, Δ*S*, and *T*Δ*S* for **S₁**-cGOx/**S₁**-cHRP bioconjugate film (at 73°C, and 170°C) and aqueous native GOx/HRP solution (at 73°C): Upon formation of the film the entropy of the system decreased considerably by approximately 774 J K^{-1} mol^{-1}, corresponding to a decrease of 267.7 kJ mol^{-1} in *T*Δ*S*, implying a significant restriction in the conformational freedom of the enzymes, resulting in a higher value of T_m within the highly concentrated (ca. 400 mg cm^{-3}) and crowded environment. An opposing contribution shown by a decrease in Δ*H* by 263 kJ mol^{-1} was also present, although this was approximately 4.7 kJ mol^{-1} (*ΔG*) less than *T*Δ*S*, which was consistent with the observations on denaturation studies for solvent-free protein liquid of myoglobin protein having a concentration of biomolecules ~280 mg cm^{-3}.[2]

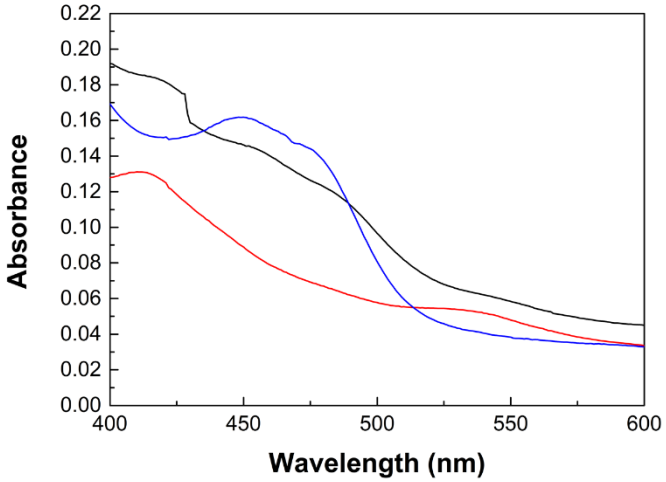

Figure S5: Diffuse reflectance UV-Vis spectra of **S_1**-cGOx/**S_1**-cHRP (black), **S_1**-cGOx (blue) and **S_1**-cHRP films (red), indicating retention of FAD and heme cofactor groups in GOx and HRP, respectively.

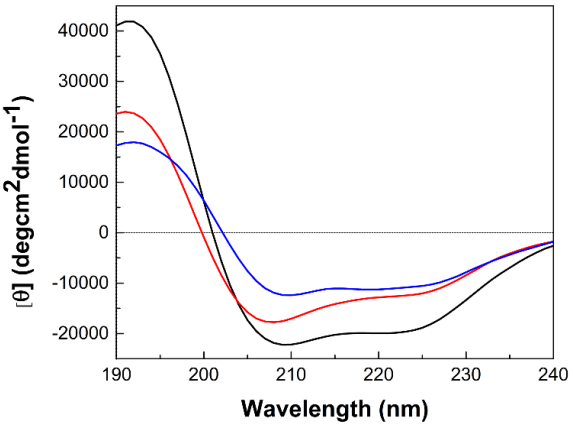

Figure S6: SRCD spectra of native (black), cationized (red) and film (blue) forms of HRP at 25°C indicates a gradual decrease in the intensity at 208 and 222 nm by 21% and 36% in aqueous cHRP, and 44% and 45% in **S_1**-cHRP dry film, relative to the native HRP, as shown in **Table S1.** This corresponded to a loss in α-helicity within the enzyme, concurrent with an increase in the unordered domains, and indicates that a significant change in the secondary structure was related to the cationization step, and that subsequent bioconjugation and crosslinking to form the film led to minimal perturbation.

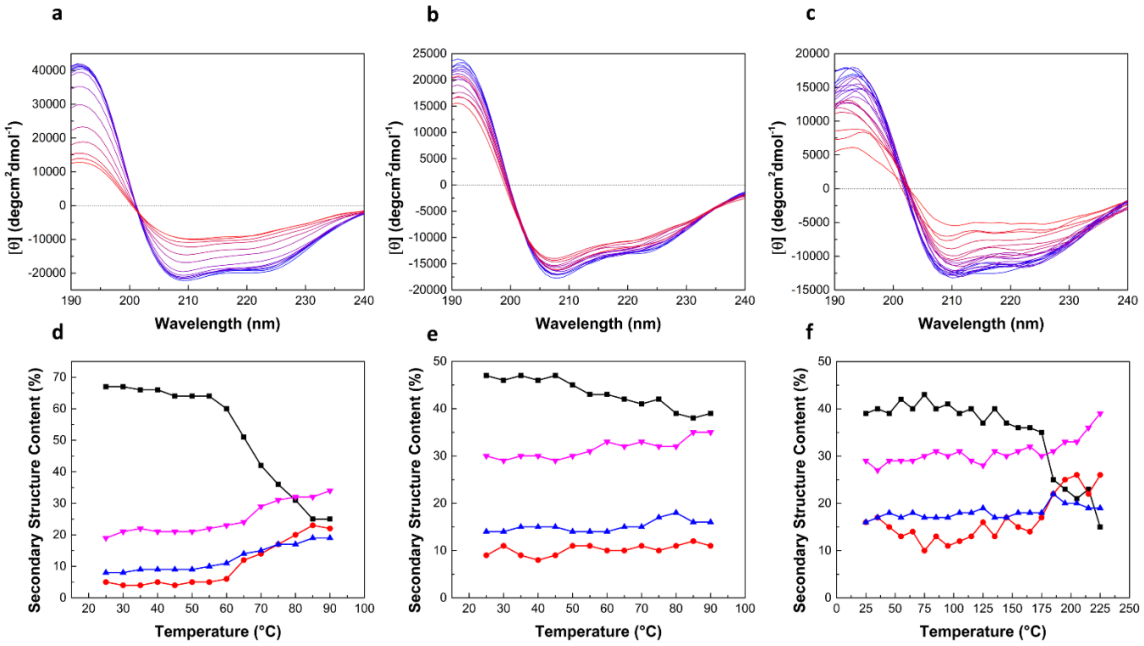

Figure S7: Temperature dependent SRCD spectra of (a) native, (b) cationized, and (c) film forms of HRP. The spectra indicated a gradual decrease in peaks at 208 and 222 nm over a temperature range of 25 (blue) to 95 or 225 (red) °C for the liquid and solid forms, respectively, as recorded at 10 °C intervals. **Figures** (d)-(f) depict the temperature dependent variation in α-helical (black squares), β-sheet (red circles), turn (blue triangles) and unordered (pink inverted triangles) domains for (d) native, (e) cationized, (f) film forms of HRP.

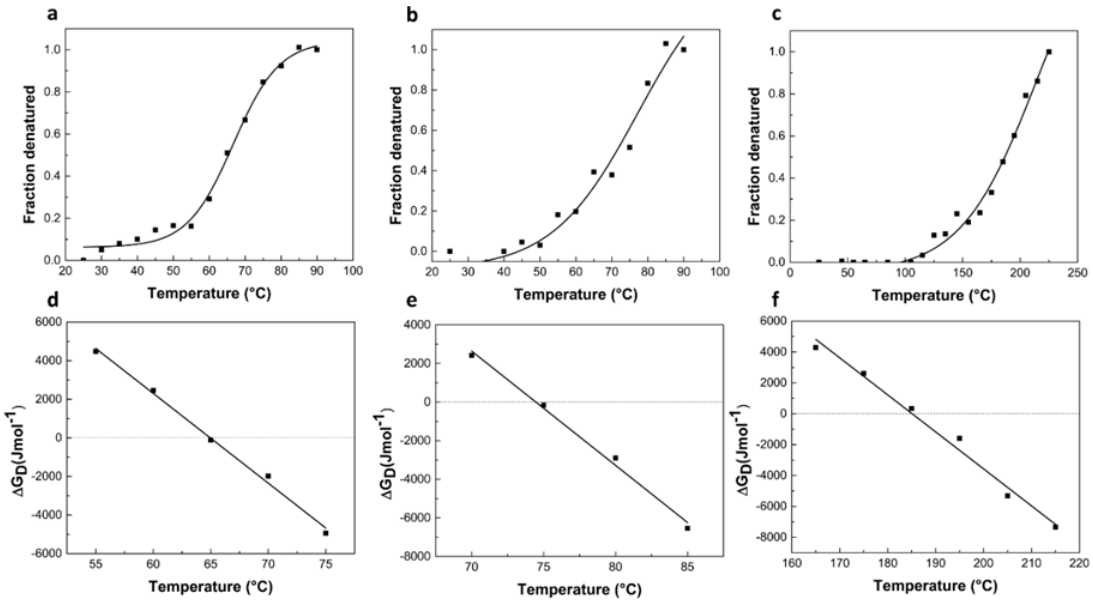

Figure S8: Plot of equilibrium fraction (peak intensity at 222 nm used) of denatured (a) native, (b) cationized, (c) film forms of HRP as a function of temperature, and their corresponding Gibbs free energy of denaturation (ΔG_D) as a function of temperature over the linear transition region (d-f). The obtained half-melting temperatures, T_m, were 64, 74 and 185 °C for the native, cationized and film forms, respectively.

Protein	Protein form	α-Helix	β-sheet	Turns	Unordered
S_1-cHRP (25°C)	Native	67 %	5 %	8 %	19 %
	Cationized	47 %	9 %	14 %	30 %
	Film	40 %	15 %	17 %	29 %

Table S3: Domain content obtained by deconvolution of the spectra for HRP enzyme in **Figure S7**. There is a gradual decrease in α-helical content on protein cationization and bioconjugation, with a corresponding increase in all other domains, indicating some structural alteration, and possibility of an α→β transition within the HRP component.

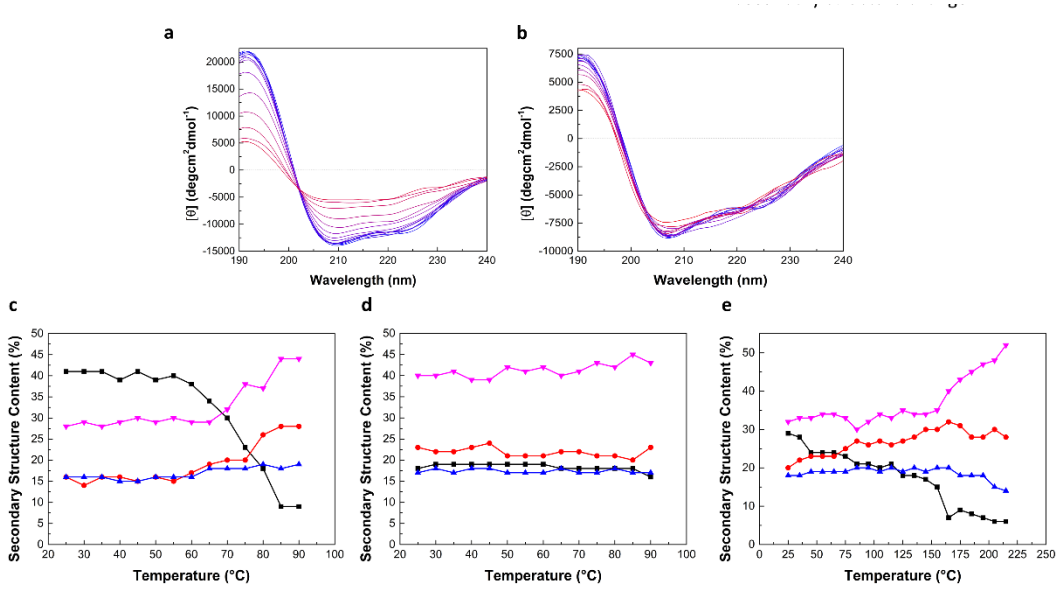

Figure S9: Temperature dependent SRCD spectra of (a) native, (b) cationized forms of GOx/HRP aqueous mixtures, showing a gradual decrease in peaks at 208 and 222 nm over a temperature range of 25 (blue) to 95 (red) °C, respectively, as recorded at 10 °C intervals. The corresponding spectrum for the two enzyme film is shown in Figure 2b. Temperature dependent variation in α-helical (black squares), β-sheet (red circles), turn (blue triangles) and unordered (pink inverted triangles) domains for (c) native, (d) cationized, (e) film forms of the GOx/HRP mixture.

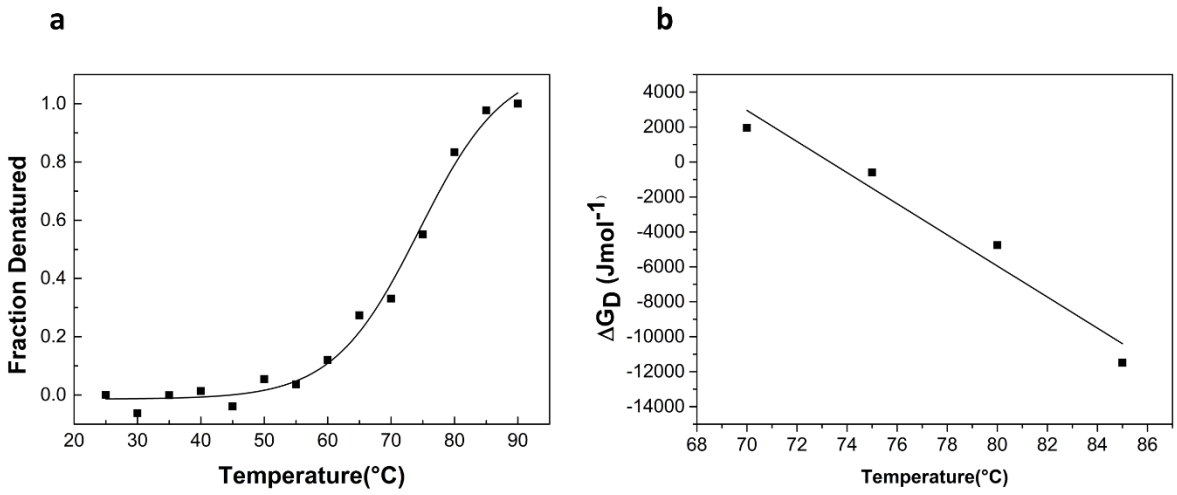

Figure S10: a) Plot of equilibrium fraction of denatured aqueous native GOx/HRP mixture as a function of temperature. b) corresponding Gibbs free energy of denaturation (ΔG_D) as a function of temperature over the linear transition region used to derive the values in Table 1.

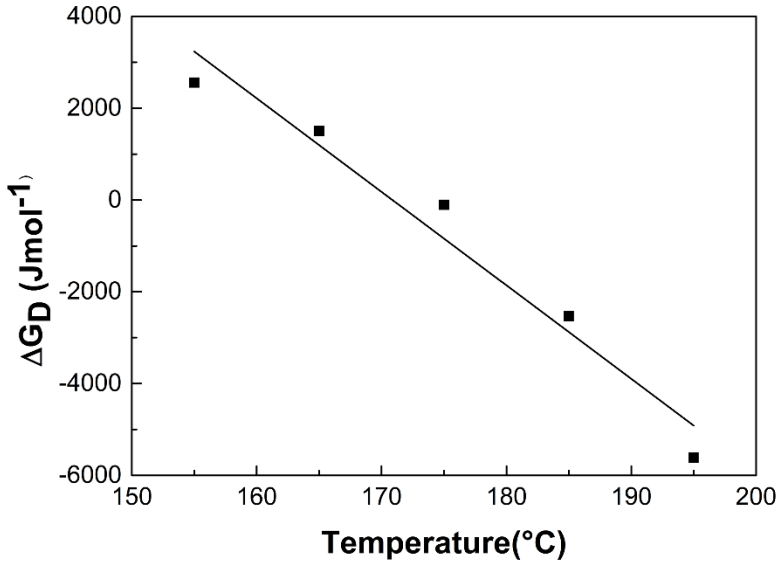

Figure S11: Plot of Gibbs free energy of denaturation (ΔG_D) as a function of temperature for the bio-conjugate **S₁**-cGOx/**S₁**-cHRP dry film. Points are taken from the linear transition within the inset plot in Figure 2c. The derived values are in Table 1.

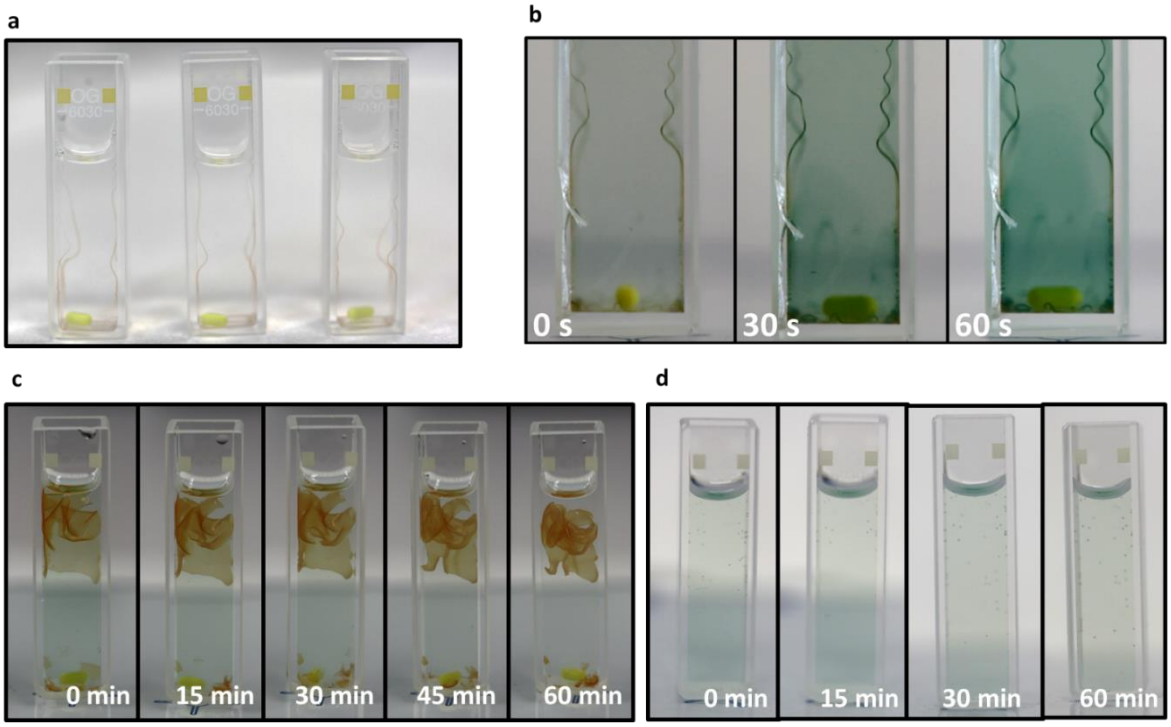

Figure S12: (a) **S₁**-cHRP films cast directly in cuvettes after hydration in water, with yellow magnetic stirrer bars at the bottom. (b) Oxidation of ABTS by a **S₁**-cGOx/**S₁**-cHrP film in the presence of 33 mM glucose. Control Experiments: (c) Time series of **S₁**-cGOx/S_1-cHRP film in the presence of phosphate buffer and ABTS. No oxidation occurs due to the absence of the glucose substrate. (d) Time series of ABTS, glucose and phosphate buffer reaction mixture used in the kinetics studies and ON-OFF experiment. No oxidation occurs since the film is not present.

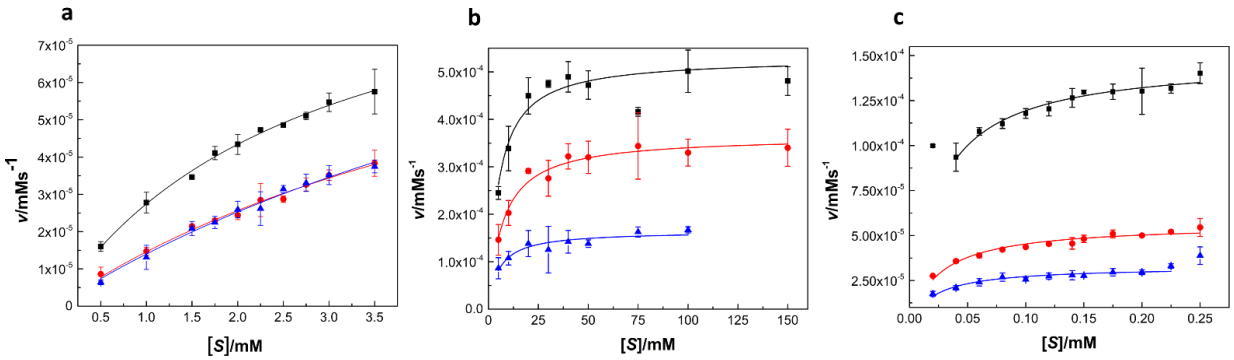

Figure S13: Michaelis Menten kinetics fits of native (black squares), cationized (red circles) and bioconjugate (blue triangles) forms of (a) BGL, (b) GOx and (c) HRP. Parameters obtained from these fits are presented in **Table S4**.

Enzyme	Substrate	Form	Michaelis Constant, K_M (mM)	Turnover number, k_{cat} (s^{-1})	Specificity constant, k_{cat}/K_m ($s^{-1}M^{-1}$)
Glucose Oxidase (GOx)	Glucose	Native	5.1 ± 0.8	59.2	11,600
		Cationized	7.2 ± 0.9	38.3	5,320
		Bioconjugates	5.1 ± 1.2	17.2	3,370
		Film	19.7 ± 3.0	0.413	20
Horseradish Peroxidase (HRP)	H_2O_2	Native	$0.023 \pm 2 \times 10^{-3}$	16.3	69,560
		Cationized	$0.024 \pm 3 \times 10^{-3}$	6.2	258,300
		Bioconjugates	$0.027 \pm 1 \times 10^{-3}$	3.9	144,400
		Film	$0.175 \pm 5 \times 10^{-2}$	0.025	142
S₁-GOx/**S₁**-HRP coupled film	Glucose	Film	20.76 ± 4.7	0.245	--

Table S4: Enzymatic parameters obtained from the Michaelis-Menten kinetics fits presented in **Figure 2b** and **Figure S13** for the different enzymatic systems used.

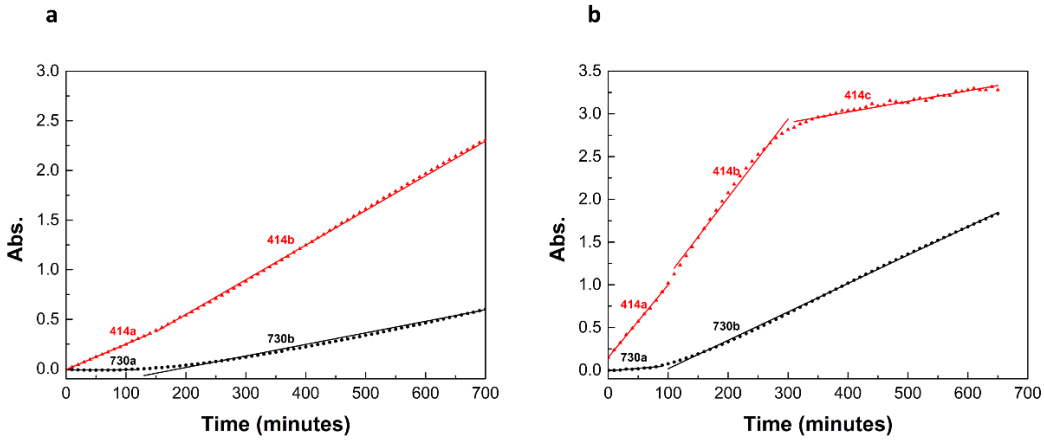

Figure S14: Time-dependent increases in absorbance at 414 nm (red) and 725 nm (black) and their linear fits for **S₁**-cBGL/**S₁**-cGOx/**S₁**-cHRP film at a) 25 °C and 37°C. Fits are made to separate areas so as to indicate differences in rates of reaction.

Wavelength (nm)	Rates of Reaction (ΔAbs.s^{-1})	
	25°C	**37°C**
414a	0.00257	0.00848
414b	0.00349	0.00918
414c	--	0.00124
730a	2.87×10^{-5}	5.99×10^{-4}
730b	0.00116	0.00332

Table S5: Values of rates of change in absorbance with time, as obtained from the corresponding linear fits in Figure S14. The values indicate that there is an overall increase in rate on increasing temperature, and that the rate at 730 nm increases significantly when the HRP catalysed step commences due to absorbance by oxidized ABTS.

3. References:

[1] B. A. Wallace, R. W. Janes, *Biochem. Soc. Trans.* **2010**, *38*.

[2] A. P. S. Brogan, G. Siligardi, R. Hussain, A. W. Perriman, S. Mann, *Chem. Sci.* **2012**, *3*, 1839.